Selection and evaluation of RFID tags and tag placement for automated inventory of containers

B. Parsons*, W. McDermott, M. Dorn, J. Strait, A. Davis, W. Saeger, A. Green, A. Roman, R. Lakis, B. Weaver, A. Cattaneo**

Los Alamos National Laboratory, Los Alamos, NM, 87545, USA

*bparsons@lanl.gov, **cattaneo@lanl.gov

Abstract

In designing radio frequency identification (RFID) systems for the automated inventory of assets, it is important to select appropriate RFID tags and methods of tag attachment to achieve a high performing and reliable system. Tag selection is especially important when designing for the unique attributes of nuclear material containers, which have constraints on tag placement, and which are often used in challenging environments for radio frequency propagation. Additionally, RFID often targets much larger applications compared to containers for nuclear materials, which influences tag design and technology trends within the industry. We will present approaches we took to identify suitable commercial off the shelf (COTS) RFID tags designed for other industries and applications and evaluate them as candidates for tagging nuclear material containers. We will cover the technical details of our approach to RFID tag selection and evaluation, as well as lessons learned from both the technical and non-technical aspects of the RFID market.

Introduction

RFID Overview

Radio frequency identification (RFID) is a set of technologies that utilize radio frequency wave communications to perform contactless identification of assets[1], [2]. RFID covers a large portion of the radio spectrum, with predominant standards for low frequency (LF) at 125/133 kHz, high frequency (HF) at 13.56 MHz, and ultra-high frequency (UHF) at 433/860-960 MHz[3]. This paper focuses on passive UHF RFID, whereby a powered transceiver—often referred to as an RFID reader—provides wireless power far field which may be harvested by an unpowered transponder—often referred to as an RFID tag—to provide power to an integrated circuit in the transponder[4]. By harvesting power from the reader, the tag may receive commands from the reader, perform limited computations and access operations, and respond back to the reader with command outputs, such as the serial number a tag has been assigned[5].

Passive UHF RFID is an attractive technology for the automated inventory of nuclear material containers. The primary advantageous features versus other types of RFID are its long range, modest reader cost, low tag cost, high tag durability, and maturity of standards and commercial off the shelf (COTS) products. Specific to nuclear material containers, these attributes provide opportunities to reduce worker absorbed dose via increasing reading distances and reduction of time in proximity to containers, while also allowing for automation of inventory tasks which would not be feasible with text or optical barcode-based systems. The maturity of the technology and its widespread use in other industries provide easy access to durable and reliable equipment that reduces the development burden. However, the unique requirements inherent to the construction of containers for nuclear materials, along with their storage and handling, present challenges that are not common to other RFID applications and which require additional research and development to address.

RFID Challenges for the Inventory of Nuclear Material Containers

The predominant challenge of UHF RFID inventory for nuclear material containers is the presence of metal, both comprising the containers as well as where containers are stored and used, such as negative pressure gloveboxes. Metal surfaces have three major impacts on UHF RFID: reflection[3], [6], [7],

multipath[8], and detuning[9]–[11]. Metal surfaces reflect incident radio frequency waves; if a metal surface is between an RFID reader and tags, the incident energy may not reach the tag to power the integrated circuit and provide a communication link unless an indirect path provides the power and communication link. Reflection may occur from both the metal enclosure as well as from nearby metal objects shielding the tag from the reader. An additional consequence of reflection is constructive and destructive interference, often termed multipath fading. When metal surfaces reflect radio waves, the distinct phases of the multiple paths between a reader and tag can combine to enhance the signal in some locations and diminish the signal in others. The multipath behavior can result in unpredictable tag reading performance as a function of location within a reading zone. Lastly, the presence of metal near the antenna of an RFID tag may detune the antenna and affect the performance of the tag. When directly in contact with metal, tags that are not designed for on-metal application may become entirely unresponsive and fail to be detected by the reader.

Overview of RFID Tags

To address the challenges described above, it is important to select RFID tags which are appropriate for the metal containers and metallic environments[12] typical to the handling and storage of nuclear materials. Standard RFID tags that are often used for retail are typically designed for application to fiberboard, plastic, and other non-metallic surfaces. On-metal tags, a subset of the market that includes tags designed for computers, tools, manufacturing equipment, and similar metal assets, are designed for application to metal surfaces. Within the on-metal tag market, there are two major design strategies: hang/flag attachment and antenna design for direct mounting on metal[13].

Hang/flag RFID tags for on-metal applications

The design principle for hang/flag RFID tags is to provide adequate space between a metal surface and the antenna of the tag to prevent performance-degrading contact with the metal surface. For hang tags, the design objective is to attach the tags using a fastener in a manner which provide sufficient free space. As demonstrated in Figure 1, hang tags require appropriate geometry to provide space for the tag to hang freely without contacting a metal surface. Mounting an example tag on the lid bolt of a 55-gallon drum provides adequate free space and the tag performs well; however, there is no suitable place to mount the same tag on a 1-quart slip top container and the tag inevitably touches metal, detuning the tag's antenna and making the tag undetectable to the RFID reader.

Like hang tags, flag tags are designed to ensure spacing between the metal surface and the antenna of the tag. Instead of hanging from a fastener, flag tags typically comprise an adhesive label that is folded to make a flag-like antenna which extends from the metal surface. Typical designs include butterfly flags, flag posts, and loop flags. Some specialized designs utilize more durable attachment methods such as screws or rivets to attach the flag tag to the assets. While flag tags can perform exceedingly well on metal assets, they remain vulnerable to antenna detuning from other nearby metal objects if the storage conditions are crowded or otherwise result in contact between the flag antenna and other metal surfaces. As demonstrated in Figure 1, a nearby metal container may touch the flag portion of the tag; in this case, anything more than slight contact between the tag and the adjacent container will detune the antenna and result in failure to read the tag. Flag antennas are also vulnerable to damage from container handling, which may tear or distort the antenna.

Direct mount RFID tags for on-metal applications

Unlike hand/flag RFID tag designs, which isolate the tag antenna from the metal surface, direct mount on-metal tags are attached directly to the metal surface and use specific packaging and antenna designs to maintain performance. On-metal tags are a recent development in the tag market and are the results of improvements to both modeling-assisted antenna design and RFID integrated circuit sensitivity. There are two major categories: soft tags and hard tags. On-metal soft tags are constructed on a flexible substrate. Most designs use a spacer between the tag antenna and the metal surface to reduce the effect

of the metal asset on the antenna tuning[14], [15]. Other recent designs use an internally folded design forming a patch antenna where the container surface extends the ground plane [16]–[18]. On-metal soft tags are economical and are compatible with commercially available RFID label printers to support print/encode-on-demand applications. On-metal hard tags have more durable construction, comprising either a specialized RFID inlay embedded in a hard matrix (e.g., thermoplastic) or a purpose-built tag using durable material such as ceramic or epoxy-glass composites with integrated antennas[19], [20]. On-metal hard tags are not compatible with print-on-demand but have increased durability to impact, vibration, and liquid exposure. Hard tags also allow more options for attaching the tag to the container, including riveting or welding, unlike soft tags which are limited to pressure sensitive adhesives.

Figure 1. (Left) An RFID hang tag mounted on a 55-gallon drum and (center) a 1-quart slip top container. (Right) An RFID butterfly-style flag tag mounted on a 1-quart slip top container with a second container touching the flag portion of the tag.

Figure 2. An example of the Sentry Slim II on-metal hard RFID tag mounted vertically on a 1-quart container. The left and center photos show the bare tag, while the right photo shows the tagged container on the left with another container in contact.

Overview of RFID Tag Placement

Three major factors must be considered in the selection of an on-metal RFID tag and its placement on the container: the dimensions of the container, the shape of the container, and how the container will be handled and utilized in a production environment. The dimensions and shape of a container naturally limit compatibility with various on-metal RFID tags. While it is obvious that a large tag may not be compatible with a small container, it is less obvious that the shape of a container may also impact tag compatibility. For example, on-metal soft tags will often specify a minimum acceptable radius of curvature to maintain the tag's antenna performance, for example a 5 cm bend radius perpendicular to the long axis of the tag[21], which limits both the minimum diameter of cylindrical containers for which the tag may be used, but also restricts the possible tag orientations. On-metal hard tags are similarly affected, with the horizontal orientation resulting in excessive gaps between the tag and the container surface which reduce tag adhesion and may also decrease RF performance. Restricting the tag orientation may also constrain the orientation of the RFID readers and result in suboptimal performance depending on the directional RF radiation pattern of the tag.

The other factor restricting tag placement is the how the container will be handled and utilized in a production environment. For example, a cylindrical container would ideally mount the RFID tag on the top of the container, which avoids bending on-metal soft tags and maximizes contact for on-metal hard tags. However, top mounting was not an option for our application for two reasons. First, some containers are considered "containers of convenience" and do not have rigorous requirements for handling of slip-top lids; lids may be swapped between containers of the same size, resulting in loss of the container-to-material association if this occurs. Second, when not in use for material storage, the containers may be vertically stacked; if the tags were top mounted on the lids, stacking would cover the tags preventing them from being detected by the reader.

Experimental

Based on the tag selection considerations described above, and initial performance testing in a free space environment, we selected the HID Vizinex Sentry Slim II (AST1-162-0300)[22], an on-metal hard tag expected to perform well in the RFID glovebox test bed, mounted in a vertical (portrait) orientation. We also selected the smallest anticipated container for our tracking application, a 1-quart slip-top metal dressing jar (PN 88010) (Medegen Medical Products). To fully evaluate the performance of the Sentry Slim II on a 1-quart container, we undertook a series of position testing experiments to understand the effects of container position within our glovebox test bed.

The glovebox test bed is a custom to-scale mock-up of a negative pressure glovebox used to handle nuclear materials, with a floor area of 64 × 52 inches, constructed using extruded aluminum supports to which aluminum panels were mounted. Like a production glovebox, the test bed has a metal interior with glass windows, glove ports, and Hypalon (chlorosulfonated polyethylene) gloves (Honeywell Safety and Productivity Solutions). To provide passive UHF capabilities to the test bed, a Zebra FX9600 4-port RFID reader (Zebra Technologies Corporation) and four Vulcan p12 +6 dBi gain right-hand circularly polarized antennas (atlasRFIDstore), were externally mounted to the glovebox. The p12 antennas were mounted on the top four windows of the glovebox with the radiating element aimed downwards; the antennas were mounted with 1-inch standoffs from the window to avoid potential effects of the window glass on the antenna tuning. To assist in the positioning of containers within the glovebox, we applied a 9 × 7 grid pattern to the interior floor of the glovebox using yellow polyvinylchloride (PVC) tape and polyethylene terephthalate (PET) labels. Each box of the grid was 8 × 8 inches. Figure 3 provides photos of the glovebox exterior and antennas, and a scale layout of the four gloveboxes in the room. Note that in addition to Glovebox 1, there is a Glovebox 2 of the same dimensions (i.e., double-side double-station gloveboxes), along with smaller Gloveboxes 3 and 4, which have a floor area of 64 × 26 inches (i.e., single-side double-station gloveboxes). Between Gloveboxes 1-2 and 3-4, there is a 64-inch-wide corridor. Between adjacent gloveboxes, there is an 18 × 15 inch metal passage that allows containers to be moved between gloveboxes, the openings of which are covered by metal panels.

Data were collected using an in-house customized version of the Zebra RFID reader host application [23] written in C# using the .NET framework. The application was modified to command the readers to report phase, channel index, antenna index, and received signal strength indicator (RSSI) for each tag read event, allowing for an in-depth analysis compared to using the default reader software or other COTS solutions we investigated. The data were collected with the parameters in Table 1.

Figure 3. (Top left) The top of Glovebox 1 showing the p12 RFID antennas mounted on the top windows. (Middle left) The front of Glovebox 1. (Bottom left) The Glovebox 1 interior during the Scenario 2 testing, with the targeted tagged container in position 4,3 (x,y). (Middle) The interior of Glovebox 1 showing the location of the p12 antenna mounted above. (Right) A cartoon showing a top-down scale view of Gloveboxes 1-4 along with the positions of the 1-quart containers placed in each glovebox. In all testing, the antennas in Glovebox 1 were powered and the container in Glovebox 1 was the targeted container.

Table 1. RFID reader parameters used for data collection on the Zebra FX9600.

Antenna settings		**RF modulation**		**Tag singulation**	
Parameter	**Setting**	**Parameter**	**Setting**	**Parameter**	**Setting**
Antennas	4	*PIE*	1.5	*Tag session*	S0
Power (dBm)	21	*TARI (μs)*	25	*Tag population*	100
Antenna dwell (s)	0.100	*Modulation type*	Miller 4	*Inventory state*	AB flip
Acquisition time (s)	60	*Baud rate (kbps)*	64	*SL flag*	SL all

We separately considered two scenarios: (1) a single tagged container placed on each grid position within Glovebox 1, and (2) a single tagged container fixed in one grid position and a second container spaced at various distances from the tag on the first container. The targeted tagged container was oriented in all tests with the tag facing the left side of Glovebox 1, as shown in Figure 3. After each container movement, the reader was started and data acquired for 60 s. The goal of Scenario 1 was to evaluate the performance of the reader and tag at each position within the glovebox, which was expected to be variable by position. The goal of Scenario 2 was to evaluate performance of the reader and tag as a function of the distance from the tag to another nearby container. In addition to the single tagged container within the glovebox in each scenario, eight tagged 1-quart containers were placed in Gloveboxes 2-4 to evaluate the effects of container movements within the monitored glovebox on spurious reads of containers in other locations.

Results and discussion

Scenario 1: Effects of position on a tagged container within the glovebox test bed

In the design of an RFID system for inside of a glovebox, we anticipated that the response of the RFID tags within the glovebox would be non-uniform between positions due to constructive and destructive interference. We also expected that the semi-directional RFID antennas needed to direct the RF beam through the windows of the glovebox would result in incomplete coverage from any single antenna.

Indeed, we observed a pattern of tag responses that is complex and is a function of container position, antenna, and channel index. Figure 4 shows the mean RSSI (averaged over the multiple per-antenna per-channel reads that occur over the 60 s acquisition period) for the targeted container at each position within Glovebox 1, faceted by antenna. Depending on the container's position and reading antenna, the RSSI ranges from–70.2 to -46.1 dBm when averaging over all 50 channels and –71.3 to -41.0 dBm when considering only channel index 25. While there are apparent trends in the spatial distribution of RSSI, as positions closer to antennas 2 and 4 having higher RSSI, it was more variable than expected. We attribute this variation to the multipath effect, where reflections within the glovebox result in constructive and destructive interference that is variable from position to position. However, averaging the tag response between all four antennas reduces the variation to a range of -62.6 to -52.1 dBm. Reviewing single channels instead of averaging, we observe that many channels exhibit null zones for which the tag is not detected at some positions for channel-antenna combinations. Figure 4 shows the heatmap of mean RSSI for channel index 25, which has multiple blank positions where the tag was not read on that antenna. However, if data from all four antennas are combined, there are no locations with zero reads. Further, the average RSSI when including all antennas is improved, ranging from -65.0 to -50.8 dBm.

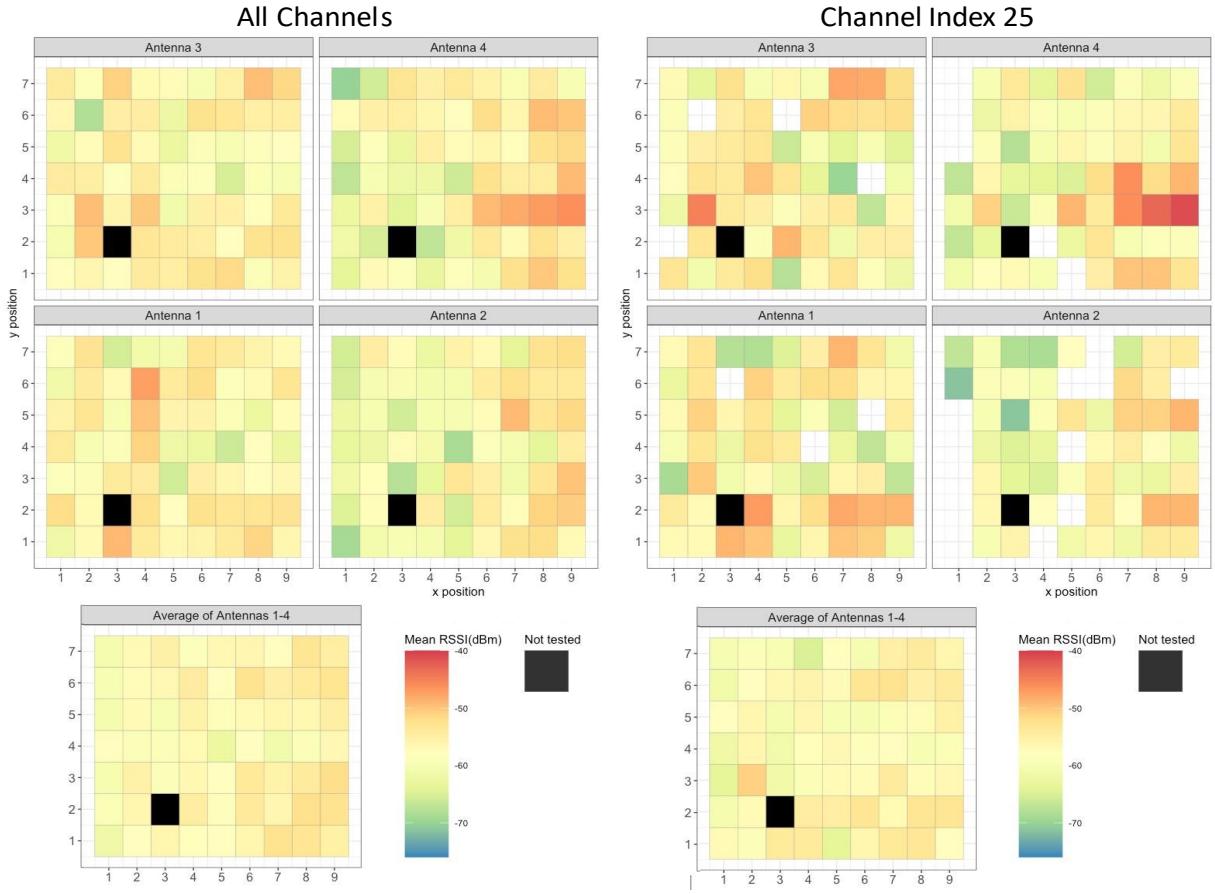

Figure 4. Heatmaps of mean RSSI as a function of container position, faceted by the antenna that read the tag on the container. (Left) Heatmaps for all channels averaged. (Right) Heatmaps for only channel index 25. (Both) Position 3,2 (x,y) was omitted due to an experimental error. The reader is referred to Figure 3 for a schematic showing the antenna locations.

We also examined RSSI variation as a function of the channel index. In FCC Part 15 (United States) RFID transmitters, 50 channels with 500 kHz bandwidth are allocated from 902 to 928 MHz, with an allowed dwell time of 0.4 seconds on each channel in a 20 second period[24]. Our customized reader software collected the channel index for each read event, allowing us to analyze the effect of the channel index on

the tag read performance. Additionally, we included the spurious tag reads from containers outside of the Glovebox 1 testbed to observe effects on selectivity. Plots summarizing these observations are provided in Figure 5, which shows the position and channel effects for true and spurious reads collected on antenna. We observe that the RSSI values are highly variable on a basis of channel index, with an average span of -13.4 dBm from the minimum to the maximum RSSI. Analyzing replicate experiments on the same position yielded repeatable RSSI values on each channel, indicating that the between-channel variation is likely a physical phenomenon related to the wavelength associated with the channel frequency and possible wavelength-dependent multipath effects, rather than variability of the reader within a given channel or between experiments.

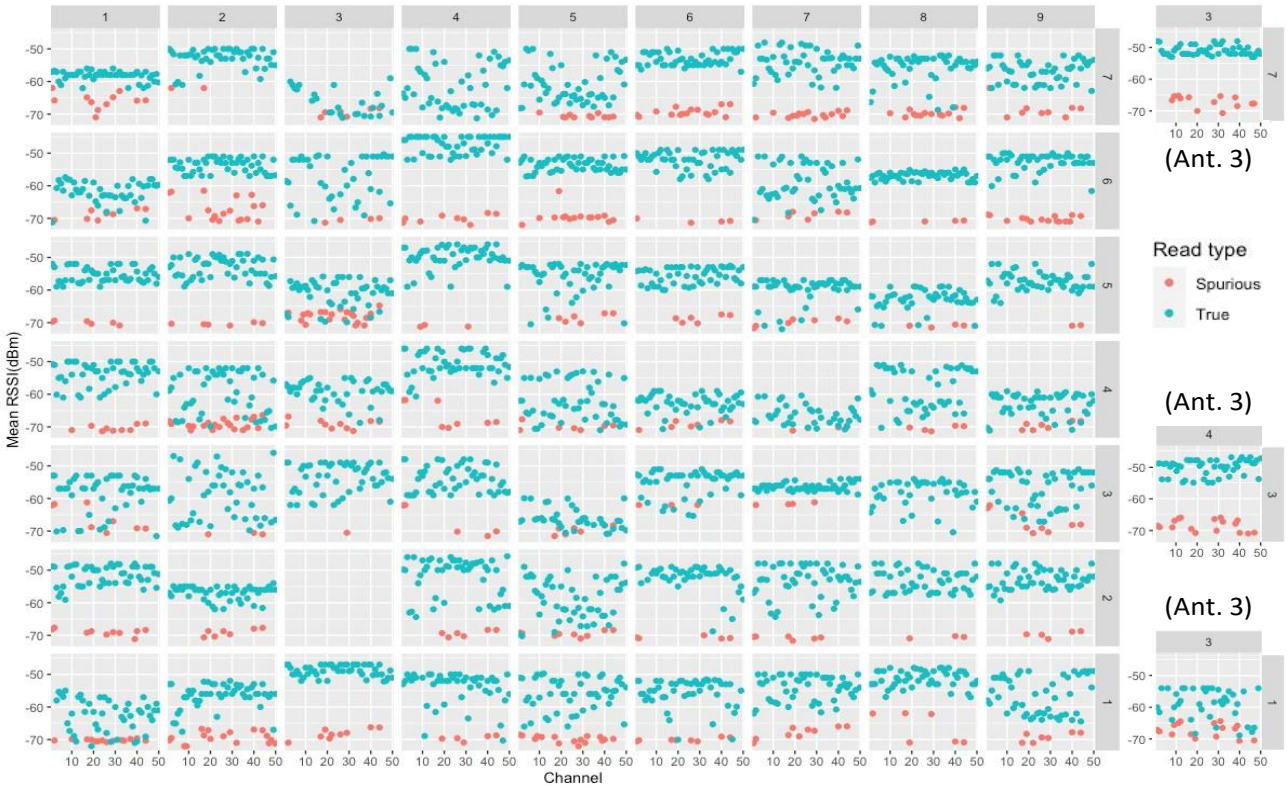

Figure 5. A scatterplot of true (targeted) tag and spurious (containers outside the glovebox) read RSSI as a function of the targeted container's position and the channel index of the read, shown for reads from Antenna 1. The inset figures in the upper right highlight the scatterplots obtained for positions 3,7; 4,3; and 3,1 (x,y) for reads from Antenna 3.

Adding additional complexity, we observe that the variation of RSSI by channel can be tightly grouped in some positions such as 1,7 (x,y) but spread in other positions, such as 5,7 (x,y). While there is no easily interpretable pattern that explains this variability from both the channel index and the position, there is clearly a phenomenon that affects the performance of the reader-tag interface. As a further consideration, we also included the mean RSSI for spurious tag reads for containers outside of the Glovebox 1 test bed. In RFID, spurious detections of tags located outside of the targeted area are often referred to a "bleed." We consider spurious reads as an indicator of the potential selectivity of the system in discriminating the true positives (i.e., tagged containers inside of Glovebox 1) from the false positives (i.e., tagged containers outside of Glovebox 1).

Scenario 2: Effects of a nearest container's distance from the tagged container

The goal of Scenario 2 was to evaluate the performance of the reader and tag on the targeted container a fixed position as a function of distance to a nearby container. For this set of experiments, we placed the targeted container in position 4, 3 (x,y) and then used a set of plastic spacers to vary the distance from the tagged container to a nearby container from 0-40 cm. The plastic spacers were used to

consistently position the containers, as this task is otherwise difficult to accomplish when working inside of a glovebox. In the 0 cm spacing, the face of the tag was in near-contact with the surface of the other container, with approximately 1 mm of free space between the two surfaces, as displayed outside of the glovebox in Figure 2 (right). Figure 6 shows the results for these experiments with RSSI plotted for all channels on antenna 3 as a function of distance between the tag and the nearby container. As expected, the tag performance is lowest when the tag is in contact with a nearby container. Conversely, the tag performance is highest when the tag is farthest from the nearby container. Indeed, when we include the data from same position in Scenario 1, shown in Figure 6 as N.C. (no additional container), we see the performance is equivalent to the Scenario 2 experiment at the 40 cm spacing. At intermediate distances, we observe an apparent interaction between the tag and the nearest container, with an apparent enhancement of RSSI at 1-3 cm of spacing versus 4-30 cm. To prevent situations where the tag is in direct contact with a neighboring container, we designed an additively manufactured ABS plastic tag cover to provide 1 cm of spacing between the tag surface and an adjacent container. In initial testing, we did not observe any detrimental effects to the tag's RF performance when the cover was placed over the tag. Figure 7 shows the cover and its application to the tag, along with a demonstration of the spacing.

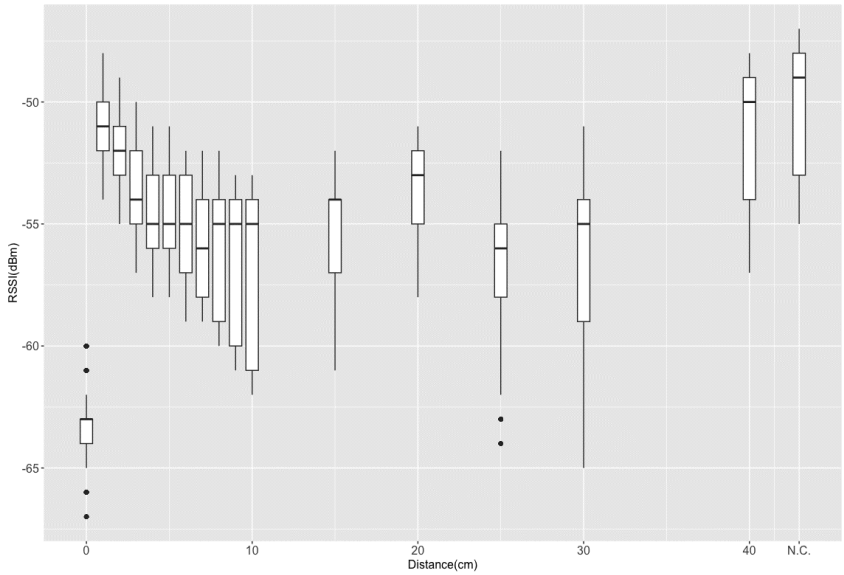

Figure 6. A box-and-whiskers plot showing the distributions of tag read RSSI for each container spacing collected in the Scenario 2 experiments, using the reads for antenna 3, which has the best sensitivity and selectivity for the position. The values shown on x-axis position N.C. are the case where there is no container, which was collected in Scenario 1.

Figure 7. (Left) the additively manufactured prototype container spacer tag cover designed for the Sentry Slim II RFID tag mounted on a 1-quart slip-top container. (Center) the tag cover installed on the container. (Right) an example of the tag cover providing spacing between the tagged container and a neighboring container.

Conclusions and future work

From our study of the passive UHF RFID tag market and initial performance testing in a glovebox testbed, we have concluded that the performance of COTS tags and readers is sufficiently high to allow for an implementation of passive UHF RFID inventory processes, even in challenging RF environments such as metal gloveboxes. Overall, this work has supported three principal findings. First, multiple antennas per glovebox are necessary to provide comprehensive coverage of the interior and avoid null zones caused by multipath interference. Second, even tags designed for on-metal mounting may be affected by proximity to other metal surfaces. However, an engineered control such as our prototype tag cover may ensure suitable container spacing to maintain tag performance. Third, the data provided by an RFID reader configured to report the tag read event metadata appears sufficiently rich to allow for algorithmic determination of various phenomena, including container presence, container movements, and changes to the glovebox environment.

Further work is planned to evaluate the performance of the system when additional containers and equipment are added to the glovebox, to better emulate realistic production environments. Additionally, we aim to further study the effects of RF parameters such as power, modulation, and session controls, and especially how selection of these parameters affects sensitivity and selectivity. We will also study the effect of multiple simultaneous readers operating on adjacent gloveboxes, which may generate interference that could require reader operation timing or frequency hopping strategies to overcome. Finally, we have planned radiation hardness testing to estimate the lifetimes possible for tags in radiation environments associated with nuclear material handling and storage.

An important limitation must be stated regarding the wide applicability of this work in the international community: regulations regarding the implementation of passive UHF RFID reader vary by country[25]. The most notable differences are the frequencies and power levels allowed for operation, though the implementation of channel usage is also a significant difference between regulated locations. Additionally, in locations where frequencies other than the 902-928 MHz spectrum are used[25], versions of RFID tags tuned to the location's UHF RFID spectrum will need to be obtained and tested, as tags tuned for other frequencies may have poor performance outside of their design range. For systems intended for use in multiple countries, efforts may be needed to both selected multi-band tags as well as to ensure performance in the different bands. In locations with limited UHF RFID spectrum allocation, the smaller number of available channels may result in different performance from this work, as we observed benefits to container detection from using multiple channels.

Acknowledgments

This work was funded by the U.S. National Nuclear Security Agency, NA-191, under the Dynamic Material Control (DYMAC) collaboration.

References

[1] A. R. Koelle, S. W. Depp, and R. W. Freyman, "Short-range radio-telemetry for electronic identification, using modulated RF backscatter," *Proc. IEEE*, vol. 63, no. 8, pp. 1260–1261, Aug. 1975, doi: 10.1109/PROC.1975.9928.

[2] J. A. Landt, R. E. Bobbett, A. R. Koelle, and P. H. Salazar, "Los Alamos Scientific Laboratory electronic vehicle identification system," Los Alamos National Lab. (LANL), Los Alamos, NM (United States), LA-7818-MS, May 1979. doi: 10.2172/6194422.

[3] D. Paret, *RFID at Ultra and Super High Frequencies: Theory and application*. Wiley, 2009. [Online]. Available: https://books.google.com/books?id=mVaQ29VT9jIC

[4] R. E. Bobbett, A. R. Koelle, J. A. Landt, and S. W. Depp, "Passive electronic identification and temperature monitoring system. Progress report, January--December 1976.," Los Alamos National Lab. (LANL), Los Alamos, NM (United States), LA-6812-PR, Jul. 1977. doi: 10.2172/7321150.

[5] "EPC(TM) Radio-Frequency Identity Protocols Generation-2 UHF RFID Standard." GS1, Jul. 2018. Accessed: Apr. 27, 2023. [Online]. Available: https://www.gs1.org/standards/rfid/uhf-air-interface-protocol

[6] P. Raumonen, L. Sydanheimo, L. Ukkonen, M. Keskilammi, and M. Kivikoski, "Folded dipole antenna near metal plate," in *IEEE Antennas and Propagation Society International Symposium. (Cat. No.03CH37450)*, Jun. 2003, pp. 848–851 vol.1. doi: 10.1109/APS.2003.1217593.
[7] M. Nikkari *et al.*, "Performance of a passive UHF RFID tag in reflective environment," in *2008 IEEE Antennas and Propagation Society International Symposium*, Jul. 2008, pp. 1–4. doi: 10.1109/APS.2008.4619587.
[8] A. Lazaro, D. Girbau, and D. Salinas, "Radio Link Budgets for UHF RFID on Multipath Environments," *IEEE Trans. Antennas Propag.*, vol. 57, no. 4, pp. 1241–1251, Apr. 2009, doi: 10.1109/TAP.2009.2015818.
[9] D. M. Dobkin and S. M. Weigand, "Environmental Effects on RFID Tag Antennas," in *IEEE MTT-S International Microwave Symposium Digest, 2005.*, Jun. 2005, pp. 135–138. doi: 10.1109/MWSYM.2005.1516541.
[10] J. D. Griffin, G. D. Durgin, A. Haldi, and B. Kippelen, "RF Tag Antenna Performance on Various Materials Using Radio Link Budgets," *IEEE Antennas Wirel. Propag. Lett.*, vol. 5, pp. 247–250, 2006, doi: 10.1109/LAWP.2006.874072.
[11] D. D. Arumugam and D. W. Engels, "Characteristics of passive UHF RFID tags on metal slabs," in *2009 IEEE Antennas and Propagation Society International Symposium*, Jun. 2009, pp. 1–4. doi: 10.1109/APS.2009.5171868.
[12] F.-K. Chen, H.-P. Lin, and T.-S. Hsu, "A Novel Approach to High Performance of RFID-Based Asset Tracking in a Metal Cabinet," in *2022 25th International Conference on Mechatronics Technology (ICMT)*, Nov. 2022, pp. 1–4. doi: 10.1109/ICMT56556.2022.9997799.
[13] T. Björninen, L. Sydänheimo, L. Ukkonen, and Y. Rahmat-Samii, "Advances in antenna designs for UHF RFID tags mountable on conductive items," *IEEE Antennas Propag. Mag.*, vol. 56, no. 1, pp. 79–103, Feb. 2014, doi: 10.1109/MAP.2014.6821761.
[14] N. Kaur *et al.*, "Design and performance of a flexible metal mountable UHF RFID tag," in *2015 IEEE 65th Electronic Components and Technology Conference (ECTC)*, May 2015, pp. 2120–2126. doi: 10.1109/ECTC.2015.7159895.
[15] D. D. Deavours, "Improving the near-metal performance of UHF RFID tags," in *2010 IEEE International Conference on RFID (IEEE RFID 2010)*, Apr. 2010, pp. 187–194. doi: 10.1109/RFID.2010.5467273.
[16] C.-W. Moh, E.-H. Lim, F.-L. Bong, and B.-K. Chung, "Miniature Coplanar-Fed Folded Patch for Metal Mountable UHF RFID Tag," *IEEE Trans. Antennas Propag.*, vol. 66, no. 5, pp. 2245–2253, May 2018, doi: 10.1109/TAP.2018.2811784.
[17] W. DENG, H. Ahokas, and M. Pylvanainen, "Rfid tag," WO2022126618A1, Jun. 23, 2022 Accessed: May 15, 2023. [Online]. Available: https://patents.google.com/patent/WO2022126618A1/
[18] S.-R. Lee, W.-H. Ng, E.-H. Lim, and S. K. A. Rahim, "Loop-Coupled Small Antenna With Enhanced Bandwidth for On-Metal UHF RFID Tag Design," *IEEE Trans. Antennas Propag.*, vol. 71, no. 4, pp. 3660–3664, Apr. 2023, doi: 10.1109/TAP.2023.3242079.
[19] K. V. S. Rao, S. F. Lam, and P. V. Nikitin, "UHF RFID tag for metal containers," in *2010 Asia-Pacific Microwave Conference*, Dec. 2010, pp. 179–182.
[20] T. C. Weakley, "Radio frequency identification (RFID) antenna with tuning stubs for mount on metal RFID tag," US8925824B2, Jan. 06, 2015 Accessed: May 15, 2023. [Online]. Available: https://patents.google.com/patent/US8925824B2/
[21] "Confidex Silverline Blade II." Confidex, 2021. Accessed: May 15, 2023. [Online]. Available: https://www.zebra.com/content/dam/zebra_dam/en/spec-sheets/confidex-silverline-blade-ii-spec-sheet-en-us.pdf
[22] "HID Sentry PCB Tag Datasheet | HID Global." https://www.hidglobal.com/documents/hid-sentry-pcb-tag-datasheet (accessed May 15, 2023).
[23] "RFID Reader Host SDK In .NET For Windows (FX Series) Support & Downloads | Zebra," *Zebra Technologies*. https://www.zebra.com/us/en/support-downloads/software/developer-tools/host-rfid-sdk-for-net.html (accessed May 15, 2023).
[24] "47 CFR 15.247 Operation of intentional RF transmitters within the bands 902–928 MHz, 2400–2483.5 MHz, and 5725–5850 MHz." Code of Federal Regulations (USA). Accessed: May 15, 2023. [Online]. Available: https://www.ecfr.gov/current/title-47/chapter-I/subchapter-A/part-15/subpart-C/subject-group-ECFR2f2e5828339709e/section-15.247
[25] "Overview of UHF frequency allocations (860 to 960 MHz) for RAIN RFID." GS1, Nov. 10, 2022. Accessed: May 15, 2023. [Online]. Available: https://www.gs1.org/docs/epc/uhf_regulations.pdf